Pathway for lipid A biosynthesis in *Arabidopsis thaliana* resembling that of *Escherichia coli*

Chijun Li, Ziqiang Guan, Dan Liu, and Christian R. H. Raetz[1]

Department of Biochemistry, Duke University Medical Center, P.O. Box 3711, Durham, NC 27710

Contributed by Christian R. H. Raetz, June 1, 2011 (sent for review March 24, 2011)

The lipid A moiety of *Escherichia coli* lipopolysaccharide is a hexaacylated disaccharide of glucosamine that makes up the outer monolayer of the outer membrane. *Arabidopsis thaliana* contains nuclear genes encoding orthologs of key enzymes of bacterial lipid A biosynthesis, including LpxA, LpxC, LpxD, LpxB, LpxK and KdtA. Although structurally related lipid A molecules are found in most other Gram-negative bacteria, lipid A and its precursors have not been directly detected in plants previously. However, homozygous insertional knockout mutations or RNAi knock-down constructs of *Arabidopsis lpx* and *kdtA* mutants revealed accumulation (or disappearance) of the expected monosaccharide or disaccharide lipid A precursors by mass spectrometry of total lipids extracted from 10-day old seedlings of these mutants. In addition, fluorescence microscopy of *lpx-gfp* fusions in transgenic *Arabidopsis* plants suggests that the Lpx and KdtA proteins are expressed and targeted to mitochondria. Although the structure of the lipid A end product generated by plants is still unknown, our work demonstrates that plants synthesize lipid A precursors using the same enzymatic pathway present in *E. coli*.

glucosamine-based lipids | Lpx genes | higher plants | electrospray ionization

Lipid A, the hydrophobic portion of LPS, is a glucosamine-based lipid that makes up the outer monolayer of the outer membrane of Gram-negative bacteria (1, 2). Kdo_2-lipid A (Fig. 1) usually represents the minimal LPS substructure required for growth (1, 2). In a few systems, like *Neisseria meningitides*, lipid A biosynthesis is not essential (3). However, in most cases lipid A biosynthesis inhibitors that target LpxC (Fig. 1) are potent Gram-negative-selective antibiotics (4). The structure of lipid A is relatively conserved in diverse Gram-negative pathogens (1, 2). Picomolar Kdo_2-lipid A is recognized by the TLR4/MD2 receptor complex of animal cells (5), triggering cytokine production that can contribute to the complications of Gram-negative sepsis (6).

Most Gram-negative bacteria encode single copy homologues of the nine *Escherichia coli* enzymes that assemble the Kdo_2-lipid A moiety of *E. coli* LPS (Fig. 1) (1, 2). Gram-positive bacteria, Archaea, fungi, insects, worms, and vertebrates do not contain these genes. Although lipid A-like molecules have not been reported in plants, many plants, including *Arabidopsis thaliana*, encode full-length nuclear orthologs of six of the nine enzymes of the *E. coli* system (Fig. 1, green asterisks; and Table 1) (1, 7). A homologue of the UDP-2,3-diacylglucosamine pyrophosphatase LpxH of *E. coli* (Fig. 1) is missing in plants, but it is also missing in some Gram-negative bacteria in which it may be replaced with a different pyrophosphatase (8).

We now report the isolation and characterization of homozygous insertional knockout mutants in the *A. thaliana* genes encoding LpxA, LpxD, LpxB, LpxK, and KdtA (Table 1 and Fig. 2). Given the presence of multiple genes encoding LpxC-like proteins in *Arabidopsis* (Fig. 2), we chose an RNAi strategy to suppress *AtLpxC* expression. Mutants generated from both gene inactivation strategies are viable under laboratory conditions. However, they accumulate (or lose) the expected lipid A precursors (Fig. 1) when analyzed by sensitive liquid chromatography–electrospray ionization/mass spectrometry (LC–ESI/MS) protocols. The lipid A biosynthetic genes of higher plants may have been acquired from Gram-negative bacteria with the endosymbiosis of mitochondria. Plant lipid A may therefore have a structural role in mitochondrial or perhaps chloroplast outer membranes. Alternatively, it may serve a regulatory role, or it may participate in signal transduction, for instance, in the plant response to infection by bacterial pathogens (9). This work definitively demonstrates the presence of lipid A precursors in a eukaryotic system.

Results

Identification of Orthologs of Lipid A Biosynthesis Genes in *Arabidopsis*. A position-specific iterated-BLAST search of the nonredundant protein sequences database was conducted using the *E. coli* protein sequences of LpxA, LpxC, LpxD, LpxB, LpxH, LpxK, KdtA, LpxL, and LpxM as probes (Fig. 1). Eleven nuclear sequences were identified in *A. thaliana*, encoding proteins with significant homology to *E. coli* LpxA, LpxC, LpxD, LpxB, LpxK, or KdtA (Table 1). Homologues of LpxH, LpxL, and LpxM were not found in *Arabidopsis*, but these are also absent in some Gram-negative bacteria (10). The *AtLpxA* gene (Table 1) encodes two mRNA splice variants, one of which directs the synthesis of a protein with two additional amino acid residues inserted in the C-terminal region. These protein variants, designated AtLpxA1 and AtLpxA2, are otherwise identical to each other; they share 38 and 37% sequence identity with *E. coli* LpxA, respectively, (Table 1), with conservation of all active site residues (11). There are five *AtLpxC* orthologs located in a 68-kb region on chromosome one (Fig. 2). They have very similar nucleotide sequences, suggesting possible gene duplications from a common ancestor. Expressed sequence tag (EST) and deduced cDNA databases indicate these *AtLpxC* genes generate at least eight different but related mRNA transcripts (Table 1). Previous studies of *E. coli* LpxC had shown that three amino acid residues (H238, D246, and H265) in the C-terminal region of the protein are critical for activity (12). These residues are truncated in two of the eight AtLpxC proteins, specifically in AtLpxC1.2 and AtLpxC5.2 (Table 1), suggesting that these two proteins are not catalytically active.

Two AtLpxD orthologs (designated AtLxpD1 and AtLpxD2) were encoded on chromosome 4 (Fig. 2 and Table 1); these proteins share 41 and 34% identity with *E. coli* LpxD (Table 1), with conservation of key catalytic residues (13); however, only AtLpxD2 contains the putative N-terminal nucleotide binding domain of LpxD (13), which is required for *E. coli* LpxD activity. Single copy genes encoding AtLpxB (AT2G04560), AtLpxK (AT3G20480) and AtKdtA (AT5G03770) (Table 1) were also found, with 31, 26, and 34% sequence identity to the corresponding *E. coli* proteins, respectively (Table 1).

Author contributions: C.R.H.R. designed research; C.L. and Z.G. performed research; C.L. and D.L. contributed new reagents/analytic tools; C.L., Z.G., and C.R.H.R. analyzed data; and C.L., Z.G., and C.R.H.R. wrote the paper.

The authors declare no conflict of interest.

[1]To whom correspondence should be addressed. E-mail: christian.raetz@duke.edu.

This article contains supporting information online at www.pnas.org/lookup/suppl/doi:10.1073/pnas.1108840108/-/DCSupplemental.

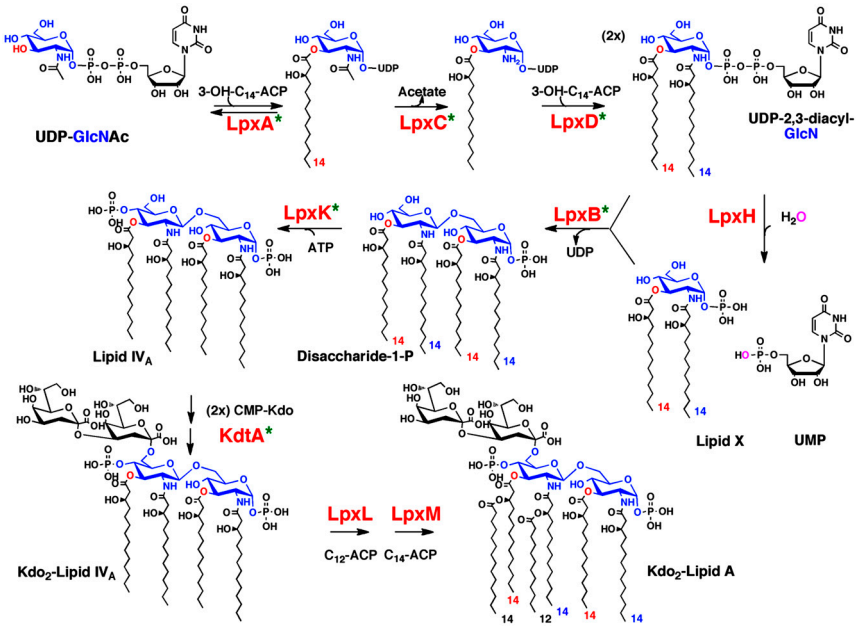

Fig. 1. Enzymatic synthesis of lipid A in *E. coli* and evidence for a similar pathway in *A. thaliana*. The green asterisks indicate that significant orthologs of the *E. coli* enzymes are present in *A. thaliana*. These proteins show 27–41% sequence identity over their full-lengths (Table 1).

Putative full-length genes encoding enzymes of lipid A biosynthesis are present in many other plants, including *Oryza sativa japonica*, *Physcomitrella patens*, *Populus trichocarpa*, *Ricinus communis*, *Selaginella moellendorffii*, *Sorghum bicolor*, *Triticum aestivum*, *Vitis vinifera*, and *Zea mays*. However, no lipid A-like molecules have previously been identified in plants by physical or chemical methods. Histochemical evidence for lipid A in green algae and peas was recently reported (14).

Insertional Knockout Mutants and RNAi Knock-Down Constructs in the Plant Lipid A System. To evaluate the functions of the putative *Arabidopsis* lipid A biosynthetic enzymes, insertional mutants for *AtLpxA*, *AtLpxD1*, *AtLpxD2*, *AtLpxB*, *AtLpxK*, and *AtKdtA* were obtained as seeds from the *Arabidopsis* Biological Resource Center at Ohio State University and other facilities (15–18) (Fig. S1). After characterizing 30-day old plants by PCR-based genotyping and RT-PCR (Fig. S2), homozygous null mutants of the above genes were identified and used for further experiments. To suppress transcription of the five closely linked *AtLpxC* genes (Fig. 2 and Table 1), independent *AtLpxC-RNAi* transgenic lines were generated in Columbia-0 (Col-0) wild-type *Arabidopsis*. In nine selected T1 transgenic lines, the expression levels of *AtLpxC* mRNA transcripts were characterized by RT-PCR using primers designed from regions of sequence identity (Fig. S2*G*, and Table S1). T3 homozygous *AtLpxC-RNAi* lines with the lowest expression of *AtLpxC* mRNA were used for further studies. All null mutants and RNAi knock-down lines were viable and showed no obvious phenotypic differences compared to wild-type plants.

Detection of 2,3-Diacylglucosamine 1-Phosphate in *Arabidopsis* and its Accumulation in an *atlpxb-1* Mutant. To detect lipid A-like molecules or lipid A precursors in *Arabidopsis*, total lipids were extracted from homogenates of 10-day old plants and subjected to normal phase LC separation coupled with online ESI/MS/MS in the negative-ion mode. In *E. coli*, 2,3-diacylglucosamine 1-phosphate (lipid X) is a key precursor of lipid A (Fig. 1). It is detectable at low levels in wild-type cells and accumulates in *lpxB* mutants (19, 20). To determine if lipid X exists in *Arabidopsis*, total lipids from the *atlpxb-1* mutant and its parental Col-0

Table 1. Full-length orthologs of *E. coli* lipid A biosynthetic enzymes in *Arabidopsis*

Gene names	Locus tags	Splice variants	Protein names	Lengths* (Ec/At)	Sequence similarity†	Paired E values	Identity (%)
AtLpxA	AT4G29540	AT4G29540.1‡	AtLpxA1	262/334	108/156/291	1×10^{-50}	38
		AT4G29540.2‡	AtLpxA2	262/336	112/157/293	3×10^{-50}	39
AtLpxC1	AT1G24793	AT1G24793.1‡	AtLpxC1.1	305/326	94/137/289	9×10^{-32}	33
		AT1G24793.2‡	AtLpxC1.2	305/266	71/109/230	1×10^{-21}	31
AtLpxC2	AT1G24880	AT1G24880.1§	AtLpxC2.1	305/369	94/138/289	1×10^{-31}	33
AtLpxC3	AT1G25054	AT1G25054.1¶	AtLpxC3.1	305/369	94/138/289	1×10^{-31}	33
		AT1G25054.2¶	AtLpxC3.2	305/326	94/137/289	9×10^{-32}	33
AtLpxC4	AT1G25145	AT1G25145.1§	AtLpxC4	305/326	94/137/289	9×10^{-32}	33
AtLpxC5	AT1G25210	AT1G25210.1¶	AtLpxC5.1	305/371	94/137/289	1×10^{-31}	33
		AT1G25210.2¶	AtLpxC5.2	305/311	71/109/230	1×10^{-21}	31
AtLpxD1	AT4G05210	AT4G05210.1¶	AtLpxD1	341/299	85/117/211	5×10^{-36}	41
AtLpxD2	AT4G21220	AT4G21220.1¶	AtLpxD2	341/304	96/144/286	5×10^{-38}	34
AtLpxB	AT2G04560	AT2G04560.1‡	AtLpxB	382/455	118/179/366	3×10^{-43}	33
AtLpxK	AT3G20480	AT3G20480.1‡	AtLpxK	328/395	88/148/336	2×10^{-27}	27
AtKdtA	AT5G03770	AT5G03770.1‡	AtKdtA	425/447	146/219/411	2×10^{-56}	36

*The full-length *E. coli* (Ec) lipid A biosynthesis proteins were compared to their predicted *A. thaliana* (At) counterparts, as currently annotated in The *Arabidopsis* Information Resource (TAIR) database. The number of amino acid residues for each protein is indicated.

†Sequence similarity is shown as identities/positives/length of aligned segments (gaps not indicated). Pairwise BLASTp alignment (40) was used to determine the E values.

‡These sequences are supported by the identification of full-length mRNA transcripts and EST records.

§These protein sequences are deduced from the genomic DNA sequences without documentation of full-length mRNA transcripts or EST records.

¶These protein sequences are deduced from the genomic DNA sequences together with some EST records.

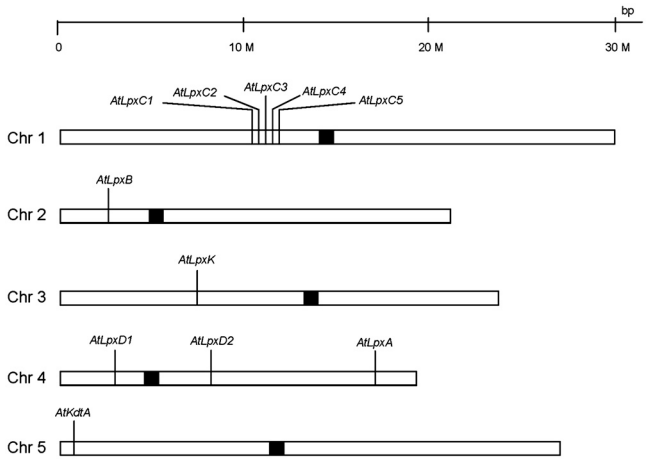

Fig. 2. Chromosomal locations of the putative *Arabidopsis* lipid A genes. The gene locations were obtained from The *Arabidopsis* Information Resource database. Multiple *AtLpxC* genes may have arisen by duplication.

wild-type plant were compared by LC–ESI/MS/MS. As shown in Fig. 3*A*, a small peak at m/z 710.43, consistent with the $[M\text{-}H]^-$ ion of a lipid X molecule bearing two *R*-3-hydroxymyristoyl chains (Fig. 1) (8, 19), was present in the wild type. It accumulated more than 10-fold in the *atlpxb-1* mutant (Fig. 3*B*). No other lipid X molecular species were detected. ESI/MS/MS analysis of the m/z 710.43 ion in the *atlpxb-1* mutant revealed the fragmentation pattern expected for lipid X (Fig. 3*C*).

To confirm the presence of lipid X and to quantify its level in the mutants (Fig. 4), a sensitive multiple reaction monitoring (MRM) protocol was developed in conjunction with LC prefractionation. Singly charged precursor/product ion pairs (710.4/240.0) were used to detect lipid X selectively (Figs. S3 and S4). The MRM peak area of the lipid X ion was normalized to that of the major species of *Arabidopsis* phosphatidylethanolamine (precursor $[M\text{-}H]^-$ ion at m/z 714.5 and product ion at m/z 279.2), which is acylated with palmitate (C16:0) and linoleate (C18:2) (Fig. S3). Lipid X accumulates 42-fold in the *atlpxb-1* mutant compared to the Col-0 wild type by this criterion (Fig. 4*A*).

Quantification of Lipid X in Other *Arabidopsis* Lipid A Mutants. The level of lipid X in the *atlpxa-1* insertion mutant was approximately 21% of its matched wild-type control [Wassilewskija (Ws)], indicating that the loss of function of *AtLpxA* did not completely eliminate the production of lipid X (Fig. 4*A*). This result implies that plants may have a second pathway for the acylation of UDP-GlcNAc not present in bacteria.

The lipid X level decreased in *AtLpxC-RNAi* transgenic plants to approximately 37% of the amount present in the Col-0 wild type (Fig. 4*A*). To confirm the function of the AtLpxC proteins in production of lipid X and the order of reactions in Fig. 1, the *AtLpxC-RNAi* transgenes were introduced into the *atlpxb-1* mutant by pollination to generate *AtLpxC-RNAi atlpxb-1* F2 homozygous plants. Fig. S5 shows that accumulation of lipid X in the *atlpxb-1* mutant was greatly attenuated by suppressing the transcription of the *AtLpxC* genes, consistent with the proposal that LpxC functions before LpxB (Fig. 1).

The lipid X level in the *atlpxd1-1* mutant was not reduced from that of wild type (Fig. 4*A*). Introducing the *atlpxd1-1* mutation into the *atlpxb-1* mutant background did not lower its elevated lipid X levels (Fig. S5). However, lipid X was undetectable in the *atlpxd2-1* mutant compared with its parental plant [Landsberg *erecta* (L*er*)] (Fig. 4*A*), indicating that AtLpxD2 is the predominant UDP-3-*O*-acyl-GlcN *N*-acyltransferase (Fig. 1). Introducing the *atlpxd2-1* mutation into the *atlpxb-1* mutant background significantly lowered lipid X levels (Fig. S5). The presence of some residual lipid X in this setting leaves open the possibility that

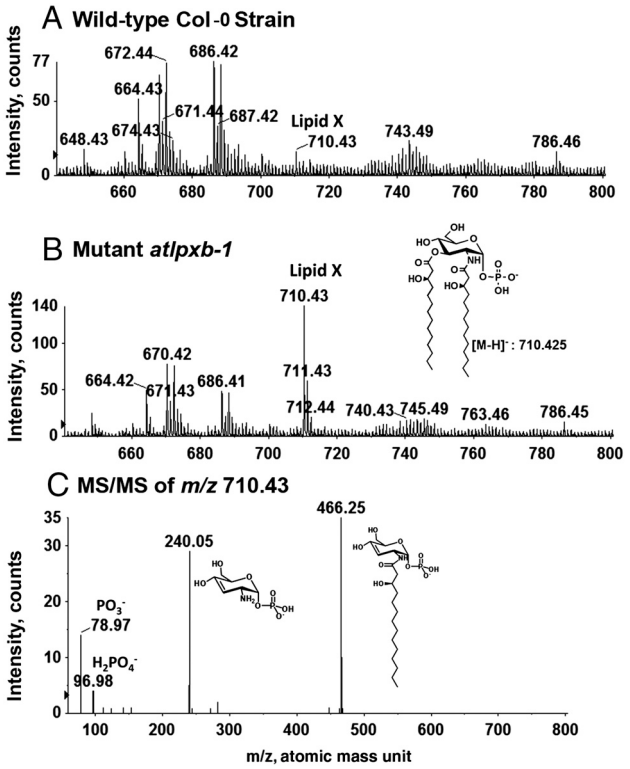

Fig. 3. Detection of the lipid A precursor 2,3-diacylglucosamine 1-phosphate in *A. thaliana*. (*A*) Negative-ion LC–ESI/MS analysis of lipids, eluting from a normal phase LC column between minutes 22.7 and 23.3, from 10-day old Col-0 wild-type seedlings. (*B*) Corresponding analysis of the lipids from 10-day old seedlings of the *atlpxb-1* mutant. The m/z 710.43 ion peak that accumulates in this mutant corresponds to the $[M\text{-}H]^-$ ion of 2,3-diacylglucosamine 1-phosphate (lipid X) with the same acyl chain composition as *E. coli* lipid X (Fig. 1). (*C*) ESI/MS/MS analysis of the lipid X $[M\text{-}H]^-$ ion at m/z 710.43, which accumulates in the *atlpxb-1* mutant. The fragment ions are the same as those seen for *E. coli* lipid X. The mass spectra were acquired using a high resolution QSTAR XL quadrupole time-of-flight tandem mass spectrometer (Applied Biosystems).

AtLpxD1 generates a small portion of the lipid X pool. In the *atlpxk-1* and *atkdta-1* mutants, lipid X levels were 2.6- and 2.2-fold higher than in the Col-0 wild type, respectively (Fig. 4*A*), consistent with the pathway (Fig. 1).

Detection of Additional Lipid A Precursors in *Arabidopsis* Mutants. UDP-2,3-diacyl-GlcN is the donor substrate for LpxB in *E. coli* (Fig. 1) (20, 21). By monitoring appropriate pairs of precursor/product ions (1,016.5/385.0) (Fig. S3), UDP-2,3-diacyl-GlcN could be detected by LC–MRM in the *atlpxb-1* mutant lipids (Fig. 4*B* and Fig. S6) at levels that are approximately 100 times lower than those of lipid X. UDP-2,3-diacyl-GlcN was not detectable in the *Arabidopsis* wild types or in any of the mutants (Fig. 4*B*).

The disaccharide-1-phosphate intermediate generated by LpxB (Fig. 1) accumulated in the *atlpxk-1* and *atkdta-1* mutants (Fig. 4*C* and Fig. S7), as judged by MRM analysis, but was not detectable in wild type or other mutant strains. Lipid IV_A (Fig. 1) was detected only in the *atkdta-1* mutant (Fig. 4*D* and Fig. S8), but was not seen in the wild type and other mutants. The independently isolated *atlpxb-2*, *atlpxk-2*, and *atlpxk-3* mutants showed similar lipid accumulation patterns as the *atlpxb-1* and *atlpxk-1* mutants.

Lipid A Pathway Enzymes are Localized in *Arabidopsis* Mitochondria. The AtKdtA protein was recently localized to mitochondria of *Arabidopsis* (22), although no characterization of its activity was reported. To determine the subcellular localization of AtLpxA,

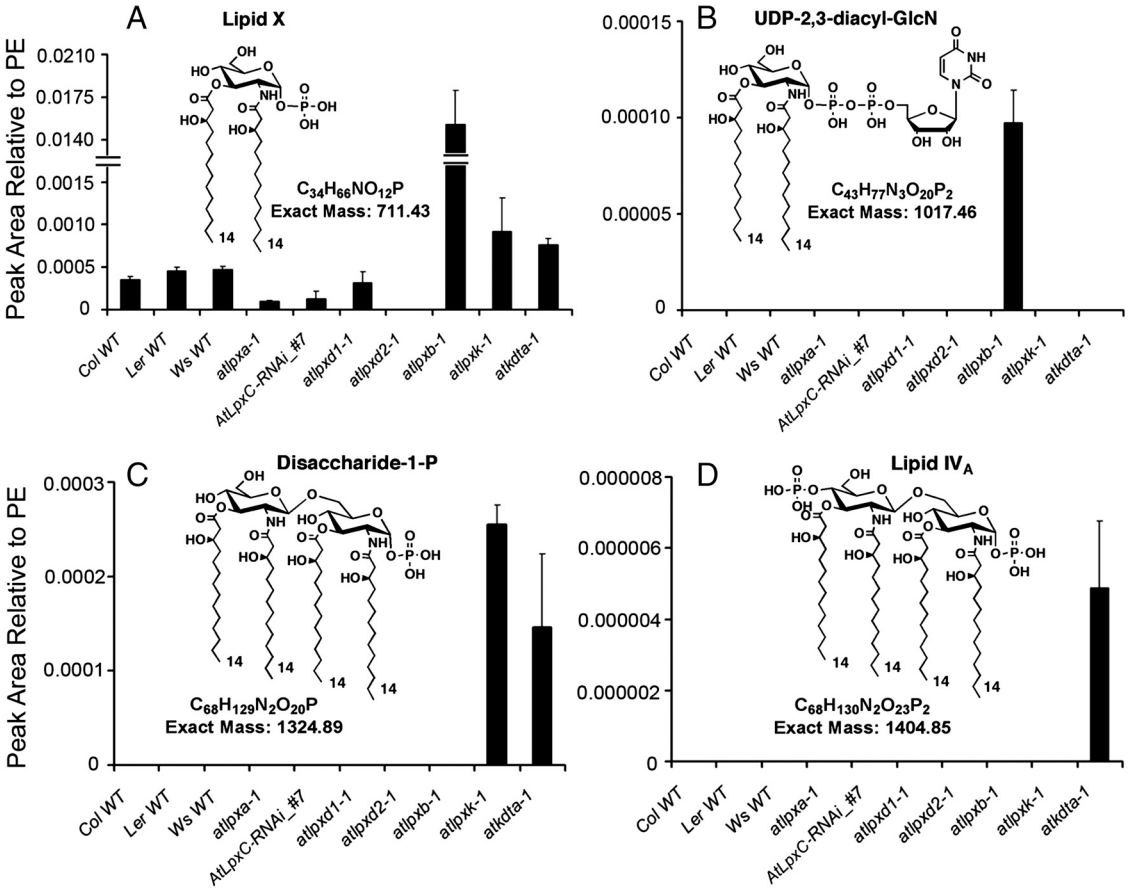

Fig. 4. Quantification of 2,3-diacylglucosamine 1-phosphate and other lipid A precursors in *Arabidopsis* mutants. MRM analysis and quantification of 2,3-diacylglucosamine 1-phosphate (lipid X) (*A*), UDP-2,3-diacyl-GlcN (*B*), disaccharide 1-phosphate (*C*), and lipid IV_A (*D*) was carried out using lipids extracted from the indicated 10-day old seedlings of three parental wild types, six *Arabidopsis* insertional mutants, and one RNAi transgenic line. These *Arabidopsis* lipid A precursors, which have the same acyl chain compositions and molecular weights as their *E. coli* counterparts (Fig. 1), were detected using the precursor/product ion pairs shown in Fig. S3. Peak areas were normalized to the major phosphatidylethanolamine molecular species (C16:0/C18:2) present in the same sample (Fig. S3). Error bars represent standard deviations of three biological replicates. The full LC–MRM tracings for each precursor/product ion pair are shown in Figs. S4, S6, S7, and S8. All LC–MRM experiments were performed using a 4,000 Q-Trap hybrid triple quadrupole linear ion trap mass spectrometer, equipped with a Turbo V ion source (Applied Biosystems).

AtLpxC1.1, AtLpxD1, AtLpxD2, AtLpxB, and AtLpxK, C-terminal GFP fusions were generated by cloning either the full-length coding sequences or the 5′ termini of the coding sequences in-frame with GFP under the control of the CaMV *35S* promoter (see *SI Materials and Methods*). These constructs were transformed into *Arabidopsis* wild-type Col-0, and T2 generation plants were analyzed by confocal microscopy. In mesophyll cells, GFP signals were shown as 1 μm dots, but were not colocalized with chloroplasts (data not shown). To avoid interference from chlorophyll auto-fluorescence, only root cells of the transgenic lines were examined. As shown in Fig. 5, the fluorescence of the GFP fusion proteins was localized to small but distinct regions. To confirm that this fluorescence reflected mitochondrial localization, MitoTracker stain (23) was used in parallel. GFP and MitoTracker fluorescence signals were recorded simultaneously. The GFP fluorescence from the full-length GFP fusions of AtLpxA and AtLpxC1.1 localized in mitochondria (Fig. 5*A*). Full-length GFP fusions of AtLpxD1, AtLpxD2, AtLpxB, and AtLpxK did not emit sufficient GFP fluorescence to permit localization. However, 5′-terminal fusions of AtLpxD1, AtLpxD2, AtLpxB, and AtLpxK to GFP showed the same mitochondrial pattern as full-length AtLpxA and AtLpxC (Fig. 5*B*).

The mitochondrial localization of the GFP fusion proteins suggested that lipid A-like molecules of plants might also be localized in mitochondria. Subcellular fractions from *atlpxb-1* plants were subjected to LC–ESI/MS. Lipid X levels in mitochondria were 3- and 48-fold higher than in chloroplasts or whole cell homogenates, respectively. Lipid X was undetectable in the plasma membrane.

Discussion

The Kdo_2-lipid A portion of LPS (Fig. 1) makes up the outer monolayer of the outer membranes of most Gram-negative bacteria (1, 2). The structure and biosynthesis of Kdo_2-lipid A are relatively conserved (1, 2). In *E. coli*, nine enzymes are required for Kdo_2-lipid A biosynthesis, designated LpxA, LpxC, LpxD, LpxH, LpxB, LpxK, KdtA, LpxL, and LpxM (Fig. 1) (1, 2). Although Kdo_2-lipid A and its precursors have not been identified previously as components of plant lipids, the emerging databases of plant protein, DNA, and EST sequences have revealed the presence of nuclear genes encoding full-length orthologs of LpxA, LpxC, LpxD, LpxB, LpxK, and KdtA in many higher plants (Fig. 1 and Table 1), including *A. thaliana*. The functions of these genes are unknown, but their presence suggests that plants synthesize lipid A-like molecules. We previously showed that *AtLpxA* can complement an *E. coli* mutant defective in its own chromosomal *lpxA* gene (1, 7), and that all active site residues of *E. coli* LpxA (11) are conserved in AtLpxA.

By combining the power of *Arabidopsis* genetics with the sensitivity of ESI mass spectrometry, we have demonstrated the presence of lipid A precursors in *Arabidopsis* with the same structures as their *E. coli* counterparts. Of the precursors shown

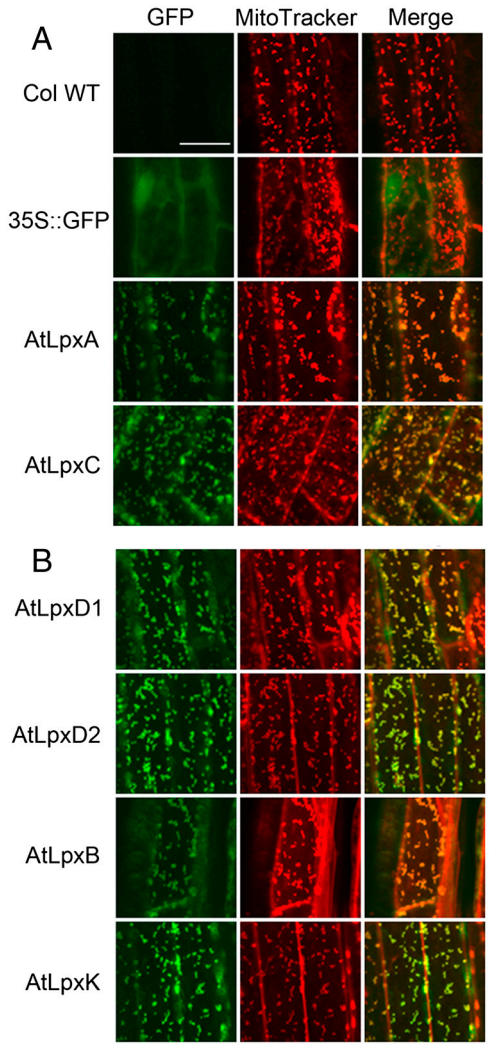

Fig. 5. Subcellular localization of GFP-fusion proteins of AtLpxA, AtLpxC1.1, AtLpxD1, AtLpxD2, AtLpxB, and AtLpxK. Roots from seven-day old *Arabidopsis* plants expressing the indicated GFP fusion proteins (green) were stained simultaneously with MitoTracker (red). The GFP and MitoTracker images were merged to show the colocalization of the GFP signal and mitochondria. Col WT, the Col-0 WT without the GFP transgene; *35S*::GFP, overexpression of GFP cDNA under the control of *35S* CaMV promoter in the Col-0 background. Scale bar: 20 μm.

in Fig. 1, only lipid X was detected in the wild type (Figs. 3 and 4). The accumulation of lipid X together with UDP-2,3-diacyl-GlcN in three independently grown *atlpxb-1* null mutant plants (Figs. 3 and 4) demonstrates that both compounds are likely substrates for AtLpxB in vivo (Fig. 1). Furthermore, the genes encoding AtLpxA, AtLpxC, and AtLpxD2 are required for the efficient production of lipid X, as judged by analyzing lipids extracted from the single null mutants or from the *AtLpxC-RNAi-7* transgenic line (Fig. 4*A*). Some residual lipid X (~21% of wild type) is present in *atlpxA* mutants (Fig. 4*A*), suggesting the presence of an additional UDP-GlcNAc acyltransferase (see below).

Five duplicated *AtLpxC* genes are found in a short region of chromosome 1 (Fig. 2 and Table 1). The lipid X level was significantly reduced (to ~37% of wild type) by suppressing *AtLpxC* gene expression with RNAi. However, it remains unclear which of the closely related AtLpxC enzymes is functional in vivo (Table 1).

Although the AtLpxD1 and AtLpxD2 proteins share more than 60% sequence identity, lipid X levels are reduced only in *atlpxd2* mutants (Fig. 4). These results suggest that AtLpxD2 is the primary UDP-3-*O*-acyl-GlcN *N*-acyltransferase in *Arabidopsis*. Our previous study of *E. coli* LpxD revealed that R293 may be required for *R*-3-OHC_{14}-ACP binding (13, 24). R293 is conserved between *E. coli* LpxD and AtLpxD2, but is replaced by lysine in AtLpxD1. AtLpxD1 also lacks two aromatic residues in its N-terminal domain that are required for acceptor substrate binding (13, 24).

At present, we cannot exclude the intriguing possibility that AtLpxD1 has LpxA activity, possibly accounting for the residual lipid X seen in *atlpxA* mutants (Fig. 4). Construction of double mutants lacking AtLpxA and AtLpxD1 should clarify this issue.

In *E. coli*, LpxK phosphorylates the disaccharide 1-phosphate product made by LpxB to generate lipid IV_A (Fig. 1) (1, 2). This step is followed by the transfer of two Kdo residues to lipid IV_A by KdtA (Fig. 1) (1, 2). The disaccharide 1-phosphate was not seen in wild-type *Arabidopsis*, but accumulates in the *atlpxk-1* and the *atkdta-1* mutants (Fig. 4*C*). Lipid IV_A is detected only in the *atkdta-1* mutant (Fig. 4*D*). We were unable to detect Kdo-lipid IV_A, Kdo_2-lipid IV_A, and putative penta- or hexa-acylated derivatives (Fig. 1). The end products of the plant lipid A pathway remain unknown. The numbers and lengths of additional acyl chains linked to Kdo_2-lipid IV_A in *Arabidopsis* might differ from those in *E. coli*, and other covalent modifications cannot be excluded (2).

The physiological role of lipid A-like molecules in *Arabidopsis* is unclear. Null mutants of *AtLpxA*, *AtLpxD2*, *AtLpxB*, *AtLpxK*, and *AtKdtA*, as well as *AtLpxC-RNAi* knock-down plants, show no obvious phenotypic differences compared to wild type under laboratory conditions, demonstrating that these genes are not essential for plant growth and development. Our investigations with GFP fusions show that the proteins required for lipid A precursor biosynthesis are targeted to the mitochondria, and the lipid X that accumulates in the *atlpxb-1* mutant is mainly located in mitochondria and chloroplasts. These findings suggest that lipid A precursors are synthesized in mitochondria and may be transported from mitochondria to chloroplasts. Conversely, plant digalactosyl-diacylglycerol is synthesized in chloroplasts, but it is found in both chloroplasts and mitochondria (25). Lipid A-like molecules of plants may serve as structural components of the outer membranes of mitochondria and/or chloroplasts, and probably were introduced by association with endosymbiotic bacteria during evolution.

Alternatively, lipid A-like molecules in *Arabidopsis* may be involved in signal transduction or plant defense responses. LPS or lipid A from some Gram-negative bacteria can induce various plant defense responses, such as an oxidative burst, NO generation, and up-regulation of pathogenesis-related genes (9, 26–31). In some cases, pretreatment with LPS helps plant cells survive subsequent attack by phytopathogens, mainly by suppressing the hypersensitive response (26, 32). Although the mechanisms by which plants detect LPS remain unknown, lipid A-like molecules in plants might serve as signals to regulate cellular responses during plant pathogen invasion.

Materials and Methods

Methods for RNA extraction and cDNA synthesis, isolation, and genotyping of insertional null mutants, plasmid constructions, and plant transformations are described in *SI Materials and Methods*. All primers used in this study are listed in Table S1.

Plant Materials and Growth Conditions. *A. thaliana* wild-type ecotypes are Col-0, Ws, and L*er*. The *atlpxa-1* mutation was in Ws background and was generated by the *Arabidopsis* Knockout Facility of the *Arabidopsis* Functional Genomics Consortium (17). The *atlpxd1-1* (CS855902) mutation was in the Col-0 background and was obtained through the University of Wisconsin-Madison (Wisconsin DsLox lines) (15). The *atlpxd2-1* (ET116191) mutation was in the L*er* background and obtained from the *Arabidopsis* Gene Trap Collection at the Cold Spring Harbor Laboratory (16). The *atlpxa-2* (SALK_092408), *atlpxa-3* (SALK_101521), *atlpxb-1* (SALK_087537), *atlpxb-2* (SALK_087529), *atlpxk-1* (SALK_063783C), *atlpxk-2* (SALK_100275C), *atlpxk-*

3 (SALK_145083), and *atkdta-1* (SALK_035981) mutations were obtained from the *Arabidopsis* Biological Resource Center and were in Col-0 background (18).

Plants were grown in long-day conditions (16 h light/8 h dark) at 22 °C in either soil or half-strength Murashige–Skoog medium (33), solidified with 0.8% agar containing 1% sucrose. For sterile growth conditions, seeds were surface-sterilized by treatment with 50% Clorox and 0.2% Triton X-100 for 10 min, and then washed five times with sterile distilled water. All seeds suspended in sterile water were kept in the dark at 4 °C for 3 d to break seed dormancy. For lipid analysis, sterilized seeds (typically 2,000) were germinated and grown for 10 d in 250 mL full-strength Murashige–Skoog liquid medium (16 h light/8 h dark), supplemented with 0.1% Plant Preservative Mixture (Plant Cell Technology, Inc.).

Subcellular Localization Experiments. To investigate the subcellular localization of the AtLpx-GFP fusion proteins, T2 generation plants of the transgenic lines were used to observe GFP fluorescence. Seven-day old seedlings grown on half-strength Murashige–Skoog plates were harvested in half-strength Murashige–Skoog medium containing 200 nM MitoTracker (MitoTracker Orange CMTMRos, Molecular Probes). After staining for 15 min, the seedlings were washed in half-strength Murashige–Skoog medium for 10 min. The seedlings were viewed with a Zeiss LSM 510 upright confocal microscope. To observe GFP and MitoTracker fluorescence simultaneously, GFP was excited at 488 nm and MitoTracker Orange at 543 nm with appropriate lasers. Fluorescence emissions were detected using BP505–530 (GFP) and LP560 (MitoTracker Orange) filters. Images were exported as digital files using the Zeiss LSM Image Browser. At least five T2 generation lines were viewed in this manner for each construct.

Plasma membranes, chloroplasts and mitochondria were isolated from 10-day old seedlings grown under sterile conditions (34–36). Protein concentration was determined by the bicinchoninic acid assay (37).

Lipid Extraction from Plant Seedlings. The 10-day old seedlings grown under sterile conditions were harvested, washed with cold distilled water, and ground with a mortar and pestle at 4 °C in a buffer (4 mL/g fresh plant weight) consisting of 0.3 M sorbitol, 5 mM $MgCl_2$, 5 mM EGTA, 5 mM EDTA, 20 mM Hepes, pH 8.0, 10 mM $NaHCO_3$, and 1% Protease Inhibitor Cocktail (P9599-5ML, Sigma). Homogenates were filtered through two layers of Miracloth (Calbiochem Ltd.). Aliquots of plant homogenates (each containing 10 mg protein in 2–3 mL) were stored at −80 °C. Lipids were extracted by the Bligh–Dyer method (38): Homogenates from wild-type or mutant plants, containing equal amounts of protein (10 mg), were diluted into 8 mL phosphate-buffered saline (39). Each 8-mL sample was extracted for 1 h at room temperature by conversion to a single phase Bligh–Dyer system, consisting of chloroform/methanol/water (1:2:0.8, vol/vol). The supernatants were collected after brief centrifugation and converted to acidic two-phase Bligh–Dyer mixtures, consisting of chloroform:methanol:0.1 M HCl (2:2:1.8, vol/vol), by adding chloroform and aqueous HCl. The lower phases were collected after low-speed centrifugation and the solvent removed by rotary evaporation. The lipids were stored at −80 °C.

LC–MRM and LC–ESI/MS/MS Detection of Lipid A Precursors in *Arabidopsis*. Detailed conditions for normal phase LC separation of total *Arabidopsis* lipids, coupled with ESI/MS/MS or MRM detection of the lipid A precursors, are provided in the *SI Materials and Methods*.

ACKNOWLEDGMENTS. The authors thank Drs. Jinshi Zhao, Hak Suk Chung, Sam Gattis, Jinhua Qian, Louis Metzger, and other lab members for helpful discussions. This research was supported by National Institutes of Health Grant GM-051310 (to C.R.H. Raetz), the Large Scale Collaborative Grant GM-069338, (to Z.G.), and the LIPID MAPS mass spectrometry facility at Duke University.

1. Raetz CRH, Whitfield C (2002) Lipopolysaccharide endotoxins. *Annu Rev Biochem* 71:635–700.
2. Raetz CRH, Reynolds CM, Trent MS, Bishop RE (2007) Lipid A modification systems in Gram-negative bacteria. *Annu Rev Biochem* 76:295–329.
3. Bos MP, Robert V, Tommassen J (2007) Biogenesis of the Gram-negative bacterial outer membrane. *Annu Rev Microbiol* 61:191–214.
4. McClerren AL, et al. (2005) A slow, tight-binding inhibitor of the zinc-dependent deacetylase LpxC of lipid A biosynthesis with antibiotic activity comparable to ciprofloxacin. *Biochemistry* 44:16574–16583.
5. Park BS, et al. (2009) The structural basis of lipopolysaccharide recognition by the TLR4-MD-2 complex. *Nature* 458:1191–1195.
6. Russell JA (2006) Management of sepsis. *N Engl J Med* 355:1699–1713.
7. Liu D, Sun TP, Raetz CRH (2003) *Arabidopsis thaliana* genes encoding orthologs of enzymes involved in *Escherichia coli* lipid A biosynthesis. *FASEB J* 17(Suppl S):A579 (abstr).
8. Metzger LE, 4th, Raetz CRH (2010) An alternative route for UDP-diacylglucosamine hydrolysis in bacterial lipid A biosynthesis. *Biochemistry* 49:6715–6726.
9. Zeidler D, et al. (2004) Innate immunity in *Arabidopsis thaliana*: Lipopolysaccharides activate nitric oxide synthase (NOS) and induce defense genes. *Proc Natl Acad Sci USA* 101:15811–15816.
10. Deckert G, et al. (1998) The complete genome of the hyperthermophilic bacterium *Aquifex aeolicus*. *Nature* 392:353–358.
11. Williams AH, Raetz CRH (2007) Structural basis for the acyl chain selectivity and mechanism of UDP-*N*-acetylglucosamine acyltransferase. *Proc Natl Acad Sci USA* 104:13543–13550.
12. Jackman JE, Raetz CRH, Fierke CA (2001) Site directed mutagenesis of the bacterial metalloamidase UDP-(3-*O*-acyl)-*N*-acetylglucosamine deacetylase (LpxC). Identification of the zinc binding site. *Biochemistry* 40:514–523.
13. Bartling CM, Raetz CRH (2009) Crystal structure and acyl chain selectivity of *Escherichia coli* LpxD, the *N*-acyltransferase of lipid A biosynthesis. *Biochemistry* 48:8672–8683.
14. Armstrong MT, et al. (2006) Histochemical evidence for lipid A (endotoxin) in eukaryote chloroplasts. *FASEB J* 20:2145–2146.
15. Woody ST, Austin-Phillips S, Amasino RM, Krysan PJ (2007) The WiscDsLox T-DNA collection: An *arabidopsis* community resource generated by using an improved high-throughput T-DNA sequencing pipeline. *J Plant Res* 120:157–165.
16. Martienssen RA (1998) Functional genomics: Probing plant gene function and expression with transposons. *Proc Natl Acad Sci USA* 95:2021–2026.
17. Krysan PJ, Young JC, Sussman MR (1999) T-DNA as an insertional mutagen in *Arabidopsis*. *Plant Cell* 11:2283–2290.
18. Alonso JM, et al. (2003) Genome-wide insertional mutagenesis of *Arabidopsis thaliana*. *Science* 301:653–657.
19. Takayama K, et al. (1983) Fatty acyl derivatives of glucosamine 1-phosphate in *Escherichia coli* and their relation to lipid A: Complete structure of a diacyl GlcN-1-P found in a phosphatidylglycerol-deficient mutant. *J Biol Chem* 258:7379–7385.
20. Bulawa CE, Raetz CRH (1984) The biosynthesis of Gram-negative endotoxin: Identification and function of UDP-2,3-diacylglucosamine in *Escherichia coli*. *J Biol Chem* 259:4846–4851.
21. Metzger LE, 4th, Raetz CRH (2009) Purification and characterization of the lipid A disaccharide synthase (LpxB) from *Escherichia coli*, a peripheral membrane protein. *Biochemistry* 48:11559–11571.
22. Seveno M, et al. (2010) Characterization of a putative 3-deoxy-D-*manno*-2-octulosonic acid (Kdo) transferase gene from *Arabidopsis thaliana*. *Glycobiology* 20:617–628.
23. Poot M, et al. (1996) Analysis of mitochondrial morphology and function with novel fixable fluorescent stains. *J Histochem Cytochem* 44:1363–1372.
24. Bartling CM, Raetz CRH (2008) Steady-state kinetics and mechanism of LpxD, the *N*-acyltransferase of lipid A biosynthesis. *Biochemistry* 47:5290–5302.
25. Jouhet J, et al. (2004) Phosphate deprivation induces transfer of DGDG galactolipid from chloroplast to mitochondria. *J Cell Biol* 167:863–874.
26. Newman MA, Daniels MJ, Dow JM (1997) The activity of lipid A and core components of bacterial lipopolysaccharides in the prevention of the hypersensitive response in pepper. *Mol Plant Microbe Interact* 10:926–928.
27. Livaja M, Zeidler D, von Rad U, Durner J (2008) Transcriptional responses of *Arabidopsis thaliana* to the bacteria-derived PAMPs harpin and lipopolysaccharide. *Immunobiology* 213:161–171.
28. Newman MA, Dow JM, Molinaro A, Parrilli M (2007) Priming, induction and modulation of plant defence responses by bacterial lipopolysaccharides. *J Endotoxin Res* 13:69–84.
29. Dow M, Newman MA, von Roepenack E (2000) The induction and modulation of plant defense responses by bacterial lipopolysaccharides. *Annu Rev Phytopathol* 38:241–261.
30. Gerber IB, Zeidler D, Durner J, Dubery IA (2004) Early perception responses of *Nicotiana tabacum* cells in response to lipopolysaccharides from *Burkholderia cepacia*. *Planta* 218:647–657.
31. Meyer A, Puhler A, Niehaus K (2001) The lipopolysaccharides of the phytopathogen *Xanthomonas campestris* pv. *campestris* induce an oxidative burst reaction in cell cultures of *Nicotiana tabacum*. *Planta* 213:214–222.
32. Sequeira L (1983) Mechanisms of induced resistance in plants. *Annu Rev Microbiol* 37:51–79.
33. Murashige T, Skoog F (1962) A revised medium for rapid growth and bioassay with tobacco tissue cultures. *Physiol Plant* 15:473–497.
34. Kubis SE, Lilley KS, Jarvis P (2008) Isolation and preparation of chloroplasts from *Arabidopsis thaliana* plants. *Methods Mol Biol* 425:171–186.
35. Millar AH, Liddell A, Leaver CJ (2001) Isolation and subfractionation of mitochondria from plants. *Methods Cell Biol* 65:53–74.
36. Santoni V (2007) Plant plasma membrane protein extraction and solubilization for proteomic analysis. *Meth Mol Biol* 355:93–109.
37. Smith PK, et al. (1985) Measurement of protein using bicinchoninic acid. *Anal Biochem* 150:76–85.
38. Bligh EG, Dyer JJ (1959) A rapid method of total lipid extraction and purification. *Can J Biochem Physiol* 37:911–917.
39. Dulbecco R, Vogt M (1954) Plaque formation and isolation of pure lines with poliomyelitis viruses. *J Exp Med* 99:167–182.
40. Altschul SF, et al. (1997) Gapped BLAST and PSI-BLAST: A new generation of protein database search programs. *Nucleic Acids Res* 25:3389–3402.